Biochemical Pharmacology 82 (2011) 287–294

Contents lists available at ScienceDirect

Biochemical Pharmacology

journal homepage: www.elsevier.com/locate/biochempharm

The effect of sphingomyelin synthase 2 (SMS2) deficiency on the expression of drug transporters in mouse brain

Yu Zhang [a], Jibin Dong [b], Xingang Zhu [a], Weirong Wang [a], Qing Yang [a,*]

[a] School of Life Sciences, Fudan University, Handan Road 220, Shanghai 200433, China
[b] School of Pharmacy, Fudan University, Zhanghen Road 826, Shanghai 201203, China

ARTICLE INFO

Article history:
Received 26 February 2011
Accepted 19 April 2011
Available online 30 April 2011

Keywords:
Sphingomyelin synthase 2
Drug transporters
Brain
ERM proteins

ABSTRACT

Sphingomyelin synthase (SMS), the last enzyme involved in the biosynthesis of sphingomyelin (SM), plays a critical role in the constitution of cell membrane and has impact on the expression of membrane proteins. SMS2, one of two SMS enzymes, is predominantly located in the plasma membrane, and is mainly expressed in the brain. Therefore, it is conceivable that SMS2 deficiency may have impact on expression of some membrane proteins, such as membrane-bound drug transporters. Using SMS2 gene deficient mouse brain tissues, we studied the gene and protein expression profiles of drug transporters, ERM proteins (ezrin/radixin/moesin) and the cytoskeleton protein, β-actin, in mouse brain by RT-PCR, western blot and immunohistochemistry analysis. We found that the mRNA expression of Mdr1 rather than the other drug transporters was significantly decreased in the SMS2 deficient brain. Accordingly, the expression and the function of Pgp (Mdr1/P-glycoprotein) were significantly downregulated in brain. In addition, the substantially downregulated expression of ezrin and β-actin was also observed in the SMS2 deficient brain. The immunohistochemistry analysis further revealed the suppressed expression of Pgp, ezrin and β-actin in both cortex and paraventricular areas of SMS2 knockout mice. Furthermore, both Pgp and β-actin were found to be co-immunoprecipitated with ezrin from the total brain lysate, suggesting the association between Pgp, ezrin and β-actin in the brain. These results indicate that SMS2 participates in the expression regulation of drug transporters, particularly Pgp, and suggest that SMS2 may be a potential target for enhancing drug access to the brain.

1. Introduction

In recent years, there has been remarkable progress in determining the pharmacological and toxicological impacts of drug transporters, which play an important role in modulating drug absorption, distribution, and elimination [1]. Drug transporters, a special family of membrane proteins, belong to two superfamilies of SLC (solute carrier) and ABC (ATP-binding cassette). While SLC transporters, characterized by 12 putative transmembrane domains, are driven by an electrochemical gradient of inorganic (or organic) solutes; ABC transporters, comprised of homologous ATP-binding and large multispanning transmembrane domains, are powered by ATP hydrolytic energy [2].

Understanding the regulation of drug transporter expression has become of great help in predicting pharmacokinetics. Recent results show that altered drug transporters expression occurs in response to signals that activate specific transcription factors, including pregnane-X receptor (PXR), constitutive androstane receptor (CAR), nuclear factor-κB and activator protein-1 [3–5]. Several other studies have demonstrated that the expression of transporters is affected by cellular stress and stress responses induced by various chemical substances and pathophysiological conditions [6–9]. Being integral membrane proteins, drug transporters are dependent on their lipid environment for their expression and optimal functions [10]. However, the effect of membrane lipids on drug transporters expression has been remained relatively unexplored.

Sphingomyelin (SM), one of the major lipids on the plasma membrane, plays an important role in determining the physical properties and biological functions of cellular membranes [11]. The last step of SM biosynthesis is catalyzed by sphingomyelin synthase (SMS) that has two isoforms of SMS1 and SMS2, which are located at golgi apparatus and plasma membrane, respectively [12]. Recent report has revealed that SMS2 deficiency inhibits sphingomyelin synthesis; thus SMS2 deficiency changes intracellular sphingomyelin accumulation and plasma membrane lipid organization [13]. SMS2 deficiency is also found to be responsible

* Corresponding author. Tel.: +86 21 65643446; fax: +86 21 65643446.
E-mail addresses: tracyzh130@yahoo.com.cn (Y. Zhang), jbdong@shmu.edu.cn (J. Dong), XingangZhu[a]082023081@fudan.edu.cn">XingangZhu[a]082023081@fudan.edu.cn (), wrwang@fudan.edu.cn (W. Wang), yangqing68@fudan.edu.cn (Q. Yang).

0006-2952/$ – see front matter © 2011 Elsevier Inc. All rights reserved.
doi:10.1016/j.bcp.2011.04.009

to significantly upregulated protein expression of ABC transporters of ABCA1 and ABCG1 in macrophage [14]. On the other hand, transporter ABCA2 deficiency caused abnormalities in the metabolism of SM in mouse brain [15]. However, the effect of SM/SMS2 on the expression of drug transporters in mouse brain has not been established.

There are increasing evidences showing that membrane-cytoskeletal linking proteins of ERM (ezrin, radixin and moesin) and the cytoskeleton protein, β-actin, are involved in the regulation of drug transporters [16,17]. The ERM deficiency was reported to be responsible to the expression and localization changes of drug transporters, such as ABCC2 in both animals and human colorectal carcinoma Caco-2 cells [18,19].

Given the brain is the organ in which the main activity of SMS and the predominant expression of SMS2 are found [12], we choose SMS2 deficient (SMS2 knockout and heterozygous) and wild type mouse brains to investigate the effect of SMS2 deficiency on drug transporters. We studied the gene expression profiles of some drug transporters, and examined the protein expression and the function of Pgp (Mdr1/P-glycoprotein) which showed significant change on its mRNA level. We also studied possible association between Pgp, ERM and the β-actin in the brain.

2. Materials and methods

2.1. Ethics statement

The Ethics Committee for Animal Experiments of Fudan University approved all animal work (permit number: SYXK 2007-0002) and the experimental protocols strictly complied with the institutional guidelines and the criteria outlined in the "Guide for Care and Use of Laboratory Animals".

2.2. Animals

Original SMS2 knockout (KO) mice were donated by Prof. XC Jiang at the Department of Cell Biology, State University of New York Downstate Medical Center, Brooklyn, and were maintained at Fudan University. The establishment of SMS2 KO mice had been previously reported by Hailemariam et al. [20]. The abbreviations for wild type, heterozygous, and SMS2 KO mice are WT, SMS2+/−, and SMS2−/−, respectively. The animals used in this study were 10–12-week-old littermates. The tissues were frozen on liquefacient nitrogen and stored at −80 °C until further use.

2.3. Reagents

SMase (S-8889), alkaline phosphatase (P5521), choline oxidase (C5896), peroxidase (P1432) and 4-aminoantipyrine (A4382) as well as phosphatidylcholine (P6638), NBD-C6-ceramide (N8278) were purchased from Sigma (St. Louis, MO, USA). DAOS (N-ethyl-N-(2-hydroxy-3-sulfopropyl)-3,5-dimethoxyaniline, sodium salt) was purchased from Dojindo Molecular Technologies, Inc. in USA. Rhodamine123 was purchased from J&K Chemical in China. Other chemicals and reagents were purchased from Sigma (St. Louis, MO, USA) or from Invitrogen (Carlsbad, CA, USA), and were of analytical grade. Antibodies were obtained from the following sources: monoclonal mouse anti-P-glycoprotein C219 antibodies from Abcam, Cambridge, UK; ACTB antibody from ProteinTech Group, USA; monoclonal anti-ezrin antibody from Thermo, USA; moesin Ab-1 (Clone 38/87) monoclonal antibody from Lab Vision, USA; monoclonal anti-GAPDH antibody from Beyotime, China; and secondary antibody labeled with alkaline phosphatase from Vecter Laboratories Inc., USA.

2.4. SMS activity assay

SMS activity was measured as described previously [21,14]. Brain tissues were homogenized in a buffer containing 50 mM Tris–HCl, 1 mM EDTA, 5% sucrose, and a cocktail of protease inhibitors (Sigma, USA). The homogenate was centrifuged at 5000 rpm for 10 min and the supernatant was mixed in assay buffer containing 50 mM Tris–HCl (pH 7.4), 25 mM KCl, NBD-C6-ceramide (0.1 μg/μL), and phosphotidylcholine (0.01 μg/μL). The mixture was incubated at 37 °C for 2 h. Lipids were extracted in $CHCl_3$:MeOH (2:1), dried under nitrogen gas, and separated by thin layer chromatography (TLC) using $CHCl_3$:MeOH:NH_4OH (14:6:1). The plate was scanned with a PhosphorImager, and the intensity of NBD-SM band was measured by Gel-Pro Analyzer 6.0 (MediaCybernetics, Inc.).

2.5. SM measurement

Mouse brain tissues (100 mg) were homogenized in 1 mL of 1 N NaOH, and the total lipids were extracted twice from the tissues with 1 mL of a $CHCl_3$:MeOH (2:1) solution. The organic layer was dried under nitrogen gas and resolubilized in 0.2 mL of $CHCl_3$ containing 2% Triton X-100. The lipid extract was dried and resuspended in 0.2 mL of water to achieve a final concentration of 2% Triton X-100. Prior to the assay for SM measurement, an enzyme solution was prepared in 50 mL of reaction buffer (Tris–HCl 0.05 M with calcium chloride 0.66 mM, pH 8) to the final concentrations of SMase 25 U, Alkaline phosphatase 500 U, Choline oxidase 25 U, Peroxidase 1000 U, DAOS 0.73 mM and 4-aminoantipyrine 0.73 mM. To 100 μL reaction buffer added 10 μL of the lipid extracts. After the reaction at 37 °C for 45 min, the absorption was measured at 595 nm on a spectrophotometric plate reader (Thermo scientific, USA) [22,23].

2.6. Reverse transcriptase-polymerase chain reaction analysis

Total RNA was isolated from the whole brain tissue using Trizol reagent (Invitrogen, Japan) according to the manufacturer's instructions. Subsequently, reverse transcription was performed using 2 μg of the RNA in a final reaction mixture (20 μL) containing random primers (12.5 ng, Invitrogen, USA), RNase inhibitor (RNaseOUT, 20 U, Takara, Japan), 0.5 mM deoxynucleotides (dNTPs, Promega, WI, USA), and 100 U of RNA reverse transcriptase (ReverTra Ace, TOYOBO, Japan). The target genes of Mdr1, Mrp1, Mrp2, Mrp3, Mrp4, Bcrp, Oatp1, Oatp2, β-actin, ezrin, radixin, and moesin as well as glyceraldehyde-3-phosphate dehydrogenase (GAPDH) were amplified with specific primers (Table 1). PCR amplifications were conducted under the following conditions: denaturation at 96 °C for 60 s, annealing at 54–60 °C for 60 s (depending on the primer), and elongation at 72 °C for 60 s (30 cycles). The PCR products were separated on 1% agarose gel and visualized by ethidium bromide staining.

To calculate the percentage changes of $mRNA_{SMS2+/-}$ or $mRNA_{SMS2-/-}$ relative to $mRNA_{WT}$ in mouse brains: the optical density of target genes was normalized with the amount of housekeeping gene GAPDH.

$$\%\ \mathrm{mRNA_{Target}} = 100\% \left\{ \frac{(\mathrm{mRNA_{Target}}/\mathrm{mRNA_{GAPDH}})_{\mathrm{SMS2\ Deficient}}}{(\mathrm{mRNA_{Target}}/\mathrm{mRNA_{GAPDH}})_{\mathrm{WT}}} \right\}$$

2.7. Western blot analysis

Whole brain tissues were resuspended in RIPA lysis buffer (50 mM Tris–HCl, pH 7.5, 150 mM NaCl, 0.1% SDS, 1% nonidet P-40,

Table 1
Sequences of PCR primers used for cloning cDNA fragments.

Primers	Accession IDs	Sequence of primer (5′–3′)	Amplicon size (bp)	Annealing (°C)
SMS2/Sgms2	NM_028943	F: GTGGCGGACAATGGATATCATAGAGACAGC R: GATAAGGTCTTGGGTTTGCCCTTGCC	145	56
Mdr1/Abcb1	NM_011076	F: CCCATCATTGCAATAGCAGG R: GTTCAAACTTCTGCTCCTGA	107	54
Oatp1/Slc21a1	NM_013797	F: GTCTTACGAGTGTGCTCCAGAT R: GGAATACTGCCTCTGAAGTGGATT	59	54
Oatp2/Slc21a5	NM_030687	F: GACGGCTCAGTGTTCATTC R: CTTCTAGCTGGTCCCTCTT	63	54
Mrp1/Abcc1	NM_008576	F: TGCGCTTCCCACTCAACATCC R: CGGGCCAGGCTCACACG	561	54
Mrp2/Abcc2	NM_013806	F: CTTGCGGTGGTCCAGTGTTTTAC R: ATGGCGAATGGCAGACCA	530	54
Mrp3/Abcc3	NM_029600	F: AGGCTGCCCGCCTGGTG R: TTCCCCACAAACTCCACAT	495	54
Mrp4/Abcc4	XM_139262	F: GAAGACAACCACAGGCCAG R: CTTGGAAATCTCCTTCTTTC	367	54
Ezrin	NM_009510	F: TAAAGCATGCCCCCACAGAGTCTCC R: AGTCACCCGCACACGACAGACATC	567	60
Radixin	NM_009041	F: TGGTGTCACACGGATCACTTACTGG R: CAGTGAAGGCCATGATTGAGACTGC	594	60
Moesin	NM_010833	F: ACAAATCTAGTCCCAGTGGGCCTTG R: CCAACCCACAGCACAATGAGTGATG	566	60
β-Actin	NM_007393	F: TCCTGTGGCATCCACGAAACT R: GAAGCATTTGCGGTGGACGAT	314	56
GAPDH	NM_008084	F: ATGGTGAAGGTCGG R: TTACTCCTTGGAGGCCATGT	1000	54

0.5% deoxycholate) containing 5 mM EDTA and protease inhibitors (PMSF, leupeptin, aprotinin) at a ratio of 100 μL buffer per 80 mg tissue. The lysate was kept on ice for 30 min, vortexed, disrupted by a 30 s burst of super sonication, and then centrifuged at 7500 rpm for 20 min at 4–8 °C. The supernatant was then collected as total proteins. Protein concentration was determined using the bicinchoninic acid method. An equal amount of proteins (50 μg) in 10 μL of SDS sample buffer was incubated at 100 °C for 5 min prior to their separation on 12% SDS-PAGE and subsequently transferring onto a PVDF membrane (Millipore, USA). The membrane was blocked with 0.5% nonfat dry milk in 0.1% PBST and then incubated with a specific primary antibody. The expression of Pgp, β-actin, ezrin, and GAPDH was, respectively, detected by 0.05 mg/mL C219 monoclonal anti-Pgp antibody, 0.2 μg/mL ACTB antibody, 1 μg/mL monoclonal anti-ezrin antibody, and 2 μg/mL monoclonal anti-GAPDH antibody. 1 μg/mL moesin Ab-1 (Clone 38/87) monoclonal antibody (antigen: 78 kDa moesin and 80 kDa radixin) was used for detection of the expression of moesin and radixin. Following overnight incubation, blots were washed and incubated for 1 h in a secondary antibody labeled with alkaline phosphatase. After washing, the blots were visualized by alkaline phosphatase buffer.

To calculate the percentage changes of $\text{Protein}_{\text{SMS2}+/-}$ or $\text{Protein}_{\text{SMS2}-/-}$ relative to $\text{Protein}_{\text{WT}}$ in mouse brains: the optical density of target proteins was normalized with the amount of housekeeping protein GAPDH.

$$\%\text{Protein}_{\text{Target}} = 100\% \left\{ \frac{(\text{Protein}_{\text{Target}}/\text{Protein}_{\text{GAPDH}})_{\text{SMS2 Deficient}}}{(\text{Protein}_{\text{Target}}/\text{Protein}_{\text{GAPDH}})_{\text{WT}}} \right\}$$

2.8. Immunohistochemistry

All animals were anesthetized with sodium pentobarbital (40 mg/kg; i.p.) and sacrificed by decapitation. The brains were rapidly dissected, fixed in the formalin–picric acid fixative (4% paraformaldehyde and 0.4% picric acid in 0.16 M phosphate buffer, pH 7) for 24 h, and embedded in paraffin. Sections (3 μm) were cut from brain specimens, deparaffinized, rehydrated, and subjected to heat induced antigen retrieval in citrate buffer (pH 6.0) for 20 min at 96 °C. After the nonspecific binding sites were blocked with serum-free blocking reagent (DAKO, Carpinteria, CA, USA), anti-Pgp antibody (1:25), anti-actin antibody (1:100), and monoclonal anti-ezrin antibody (1:100) was, respectively, applied for 4 h at 25 °C. Immunodetection was carried out with Envision reagent (antimouse-HRP; DAKO) for 30 min. 3,3-Diaminobenzidine was then used as the visualizing substrate. Finally, the sections were counterstained with hematoxylin. To rule out false positive staining due to unspecific binding of antibodies, control samples were prepared under the same conditions with the primary antibody of isotype-matched IgG.

2.9. Immunoprecipitation

Whole brain tissues of wild type mice were mixed with 0.25 mL of RIPA buffer (50 mM Tris–HCl, 150 mM NaCl, 1% Nonidet P-40, 0.5% cholic acid, pH 8.0). Ezrin was immunoprecipitated from the tissue lysates with mouse monoclonal antibody ezrin/p81/80 K for 3 h at 4 °C. To each immunoprecipitated sample, 20 μL of the mixture of Protein A/G Sepharose beads (York Biotech, China) was added and gently rocked at 4 °C for 2 h. Next, the beads were collected and washed twice in 1 mL of RIPA buffer and once in PBS. The beads were then resuspended in Laemmli sample buffer and boiled at 100 °C for 5 min. The proteins containing in the supernatants were separated by 12% SDS-PAGE, blotted to a PVDF membrane, and applied to western blot analysis.

2.10. Pgp function determination

Pgp function in mouse brain was assessed by measuring the brain-to-plasma concentration ratio of rhodamine123, which is a well known Pgp substrate. The mice were sacrificed under light ether anesthesia at 45 min following i.v. (tail vein) administration of rhodamine123 (0.2 mg/kg), and the whole brain and blood samples were taken. Whole brain tissues were resuspended in purified water at a ratio of 100 μL per 80 mg tissue, homogenized and then centrifuged at 12,000 rpm for 5 min. The blood samples were centrifuged at 12,000 rpm for 5 min. The supernatant from both brain tissue and blood was

then respectively collected, and subjected to fluorescent measurement. The fluorescent rhodamine123 was measured at $\lambda_{excitation}$ 500 nm and $\lambda_{emission}$ 543 nm using a Synergy HT microplate reader (BioTek Instruments, Inc., Winooski, VT USA). Brain accumulation of rhodamine123 was normalized by the tissue weight and rhodamine123 added (total intensity), while blood accumulation of rhodamine123 was normalized by the blood volume and rhodamine123 added (total intensity) [24].

2.11. Statistical analyses

Statistical analyses were done with SPSS Statistics V17.0 software. Experiments in triplicate were repeated 2 or more times in tissue models. The results represent the means ± SD. Student's *t*-test was performed to compare mean values.

3. Results

3.1. Phenotype of SMS2 deficient mice

SMS2 KO mice were established by conventional approaches and the resulting heterozygous mice were crossed. SMS2 KO and heterozygous mice displayed no obvious abnormalities compared to wild type mice, grew into adulthood, and bred normally under a general diet and environment. In order to confirm the SMS2 deficiency, RT-PCR analysis of SMS2 mRNA expression in WT, SMS2+/− and SMS2−/− mouse brain was performed. As expected, SMS2 mRNA was not detected in the brains of SMS2 KO mice (Fig. 1A).

3.2. The effect of SMS2 deficiency on SMS activity, SM levels in mouse brain

As expected, the SMS activity was reduced by 14% in SMS2+/− mice and 17% in SMS2−/− mice ($p < 0.05$), respectively, compared to the wild-type mice (Fig. 1B). We next sought to measure the SM levels in SMS2 deficient mouse brain. As shown in Fig. 1C, the SM levels in SMS2+/− and SMS2−/− mice were significantly reduced by 20% and 25%, respectively ($p < 0.01$). These results confirmed that the SMS2 is responsible for the regulation of SMS activity and SM levels in mouse brain.

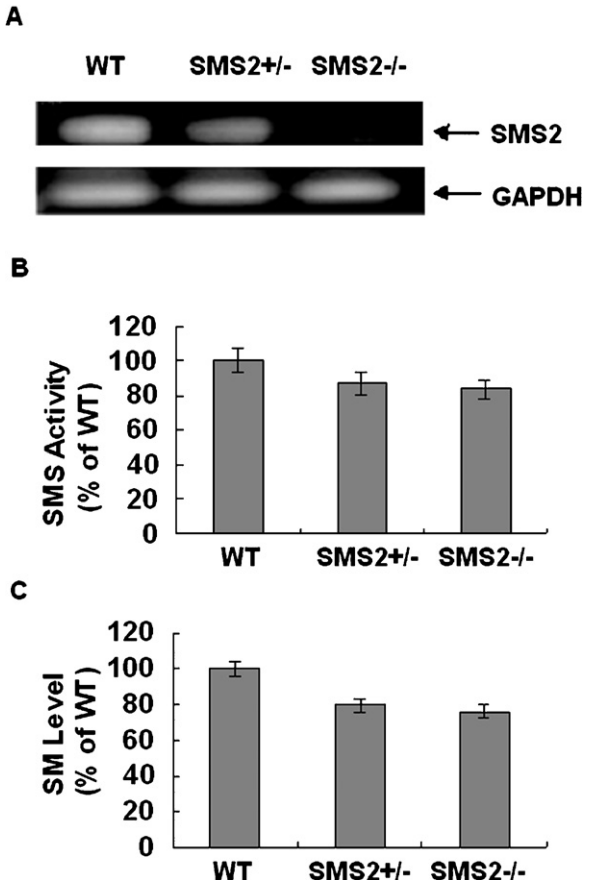

Fig. 1. Evaluation of SMS2 mRNA expression, SMS activity and SM levels in WT, SMS2+/− and SMS2−/− mouse brains. The abbreviations of WT, SMS2+/−, and SMS2−/− are used for wild type, heterozygous, and SMS2 KO mouse brains, respectively. (A) In SMS2+/− and SMS2−/− mouse brains, SMS2 mRNA had less or lost expression, GAPDH was shown as an internal reference gene for the amplification of cDNAs. (B) The effect of SMS2 deficiency on SMS activity. Values from three independent experiments are presented as means ± standard deviation (SD), $^{*}p < 0.05$. (C) The effect of SMS2 deficiency on SM levels. Values from three independent experiments are presented as means ± standard deviation (SD), $^{*}p < 0.05$.

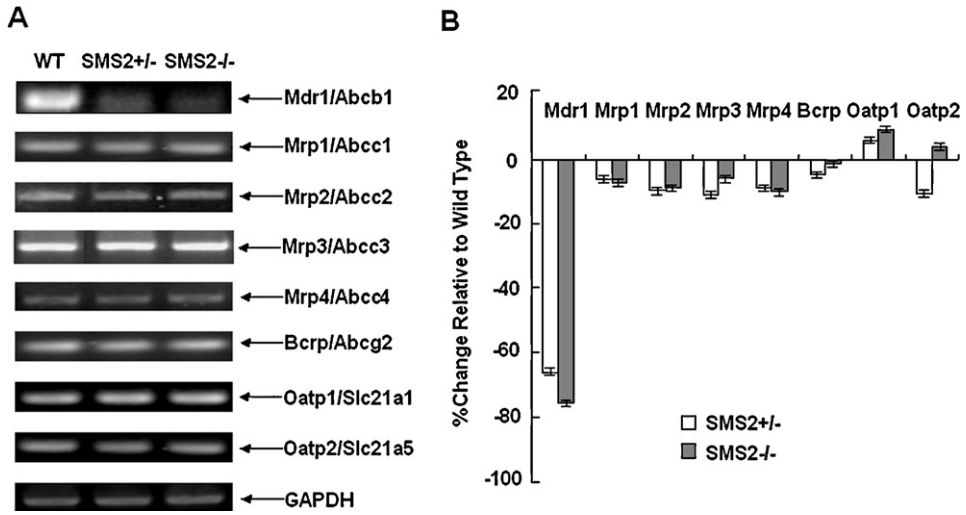

Fig. 2. mRNA expression profiles of drug transporters in WT, SMS2+/− and SMS2−/− mouse brains. (A) Agarose gel images of the eight transporter genes (Mdr1, Mrp1, Mrp2, Mrp3, Mrp4, Bcrp, Oatp1, and Oatp2) and a housekeeping gene (GAPDH). (B) Expression changes of the mRNA expression of drug transporters in the SMS2 deficient brains relative to those in the wild type brain. Values from three independent experiments are presented as means ± standard deviation (SD), $^{*}p < 0.05$.

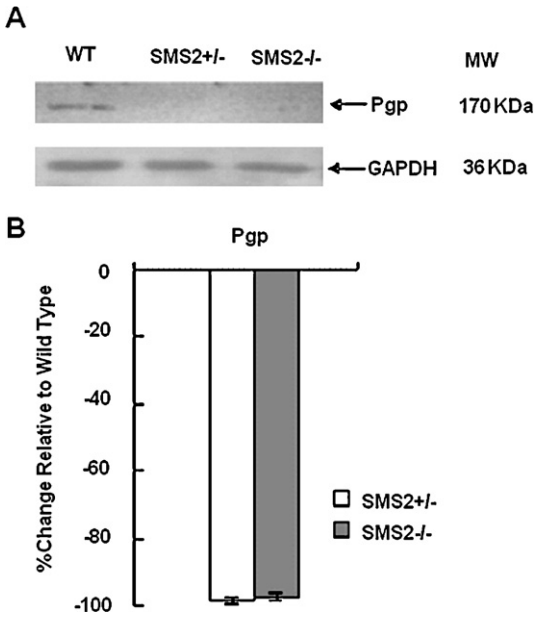

Fig. 3. Protein expression profiles of Pgp in WT, SMS2+/− and SMS2−/− mouse brains. (A) Western blot images of the Pgp and GAPDH proteins. (B) Expression changes of Pgp in the SMS2 deficient brains relative to that in the wild type brain. Values from three independent experiments are presented as means ± standard deviation (SD), * $p < 0.05$.

3.3. Effects of SMS2 deficiency on drug transporter mRNA expression

To determine whether SMS2 deficiency affects the gene expression of drug transporters in mouse brain, the mRNA of Mrp1, Mrp2, Mrp3, Mrp4, Bcrp, Oatp1, and Oatp2 was amplified with each specific pairs of primers (Table 1) from the total RNA isolated from the brains. The mRNA expression profiles of these transporter genes were shown in both agarose gel images (Fig. 2A) and a graph (Fig. 2B). The percentage changes of transporter mRNA expression in either SMS2+/− or SMS2−/− mouse brain relative to that in the wild type brain (Fig. 2B) were calculated in view of the optical densities of corresponding bands in the gels (Fig. 2A). Except Mdr1, the mRNA expression levels of the other seven transporters in either SMS2+/− or SMS2−/− mouse brain were comparable to those in the wild type brain (Fig. 2B). However, about 70–80% downregulated expression of Mdr1 was observed in both heterozygous and SMS2 KO mouse brains (Fig. 2B). These results suggested that Mdr1 was much more sensitive to SMS2 deficiency than the other seven drug transporters in mouse brain.

3.4. Effect of SMS2 deficiency on Pgp protein expression

To further investigate the effect of SMS2 deficiency on the protein expression of Pgp encoded by Mdr1 gene, the total proteins were isolated from the mouse brains and an equal amount of the proteins (50 μg) was applied to western blot analysis (Fig. 3A). As shown in Fig. 3B, the expression of Pgp was significantly downregulated in the brains of heterozygous and SMS2 KO mice. These results are consistent with Mdr1 expression in the brains (Fig. 2B).

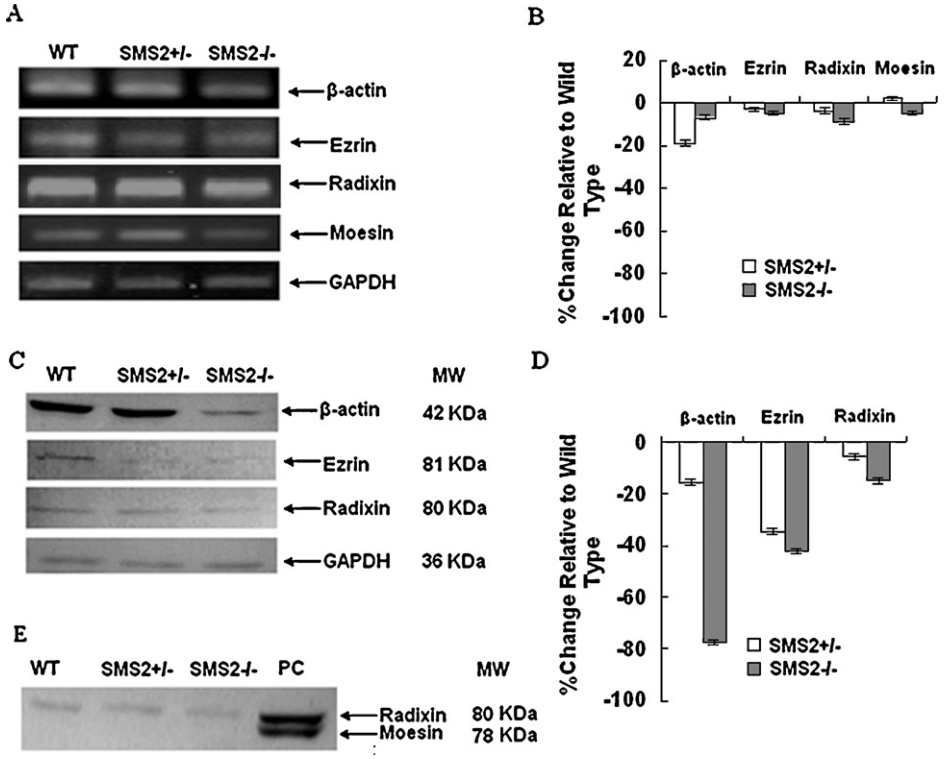

Fig. 4. ERM and β-actin expression profiles in WT, SMS2+/− and SMS2−/− mouse brains. (A) mRNA expression of ERM and β-actin evaluated by RT-PCR. (B) Expression changes of ERM and β-actin in the SMS2 deficient brains relative to those in the wild type brain. Values from three independent experiments are presented as means ± standard deviation (SD), *$p < 0.05$. (C) Western blot images of ezrin, radixin, moesin and β-actin expression. *Note*: Although moesin Ab-1 (Clone 38/87) monoclonal antibody (Lab Vision, USA) can detect both moesin (78 kDa) and radixin (80 kDa); only radixin was found in the samples. The expression deficiency of moesin in the brains was verified in an additional western blot image shown in (E). (D) Expression changes of ERM and β-actin in the SMS2 deficient brains relative to those in the wild type brain. Values from three independent experiments are presented as means ± standard deviation (SD), *$p < 0.05$. (E) Western blot image of radixin and moesin expression. PC is the total protein of human SGC-7901 cells, which express all ERM proteins of ezrin, raxidin and moesin.

3.5. Effects of SMS2 deficiency on ERM and β-actin expression

To address whether SMS2 deficiency affects the gene expression of ERM, the mRNA of ezrin, radixin, and moesin was amplified with each specific pairs of primers (Table 1), and an equal amount of the RT-PCR products was loaded to the gel. Among three ERM genes, the mRNA expression level of moesin was substantially less than those of ezrin and radixin in the mouse brain (Fig. 4A and B). However, the difference between corresponding protein expression of ERM was much pronounced (Fig. 4C and D), in which the expression of moesin (78 kDa), just below the radixin (80 kDa) was hardly detected. The expression deficiency of moesin in the brains was further verified by an additional western blot analysis (Fig. 4E) including a positive control (PC), which is the total protein of human SGC-7901 cells expressing all ERM proteins. Moreover, as shown in Fig. 4D, ezrin was affected more than radixin by SMS2 deficiency. Specifically, ezrin expression was decreased in both SMS KO and heterozygous mouse brains to about 37–43%; while radixin expression was reduced less than 10–20%.

Before GAPDH was selected as an internal reference for the western blot analysis of Pgp expression, the β-actin was initially used. Nevertheless, less than 10% suppression of β-actin mRNA expression was found in the SMS2 KO brain (Fig. 4A and B); up to 70% downregulated expression of β-actin protein in SMS2 KO mouse brain was revealed in the western blot image (Fig. 4C and D). These results suggested that SMS2 KO affects the β-actin in its protein expression more than its gene expression in mouse brain.

3.6. Comparison between the brain specimens of SMS2 KO and wild type mice: relative expression of Pgp, ERM and β-actin

To verify the expression difference of Pgp, ERM and β-actin in the SMS2 KO mouse brain from the wild type, the cerebral cortex and paraventricular areas of the brains were dissected and applied to immunohistochemistry analysis. As shown in Figs. 5 and 6, the presence of Pgp, ezrin, and β-actin proteins was revealed by 3,3′-diaminobenzidine as chromogen and corresponding immunostaining in both the cortex and paraventricular areas. In consistent with the western blot analysis, the expression of Pgp in the cortex and paraventricular areas of SMS2 KO mouse brain was obviously decreased compared to that in the wild type samples. Similarly, the immunohistochemistry images of ezrin and β-actin revealed that their immunostaining intensities were much weaker in both the cerebral cortex and paraventricular areas of SMS2 KO mouse brain compared to those in the wild type samples (Fig. 6). Taken together, both western blot and immunohistochemistry analysis results demonstrated that the expression levels of Pgp, ezrin, and β-actin were all significantly reduced in SMS2 deficient mouse brain. These results suggested that there might be a close interaction among these three proteins. To confirm this hypothesis, co-immunoprecipitation analysis of Pgp, ezrin, and β-actin was carried out. As shown in Fig. 7, both Pgp and β-actin were found to present in ezrin immunoprecipitatd protein sample, indicating that Pgp and β-actin were associated with ezrin in mouse brain.

3.7. Effect of SMS2 deficiency on Pgp function in mouse brain

To determine the effect of SMS2 deficiency on Pgp function in mouse brain, the brain distribution of rhodamine123 was examined. The mice were sacrificed at 45 min following i.v. (tail vein) rhodamine123 (0.2 mg/kg), and the brain and the blood samples were taken. Table 2 presented the rhodamine123 distribution results. The brain-to-plasma concentration ratio of rhodamine123 in the SMS2 KO was nearly eight-fold bigger than that in the WT brain. These results demonstrated that in SMS2 deficient mouse brain, the accumulation of rhodamine123, a well known substrate of Pgp, is significantly increased, and indicated that the P-glycoprotein function was inhibited. The inhibited Pgp function might be resulted from the underexpression of Pgp due to the downregulation of Mdr1 gene in SMS2 deficient mice brain.

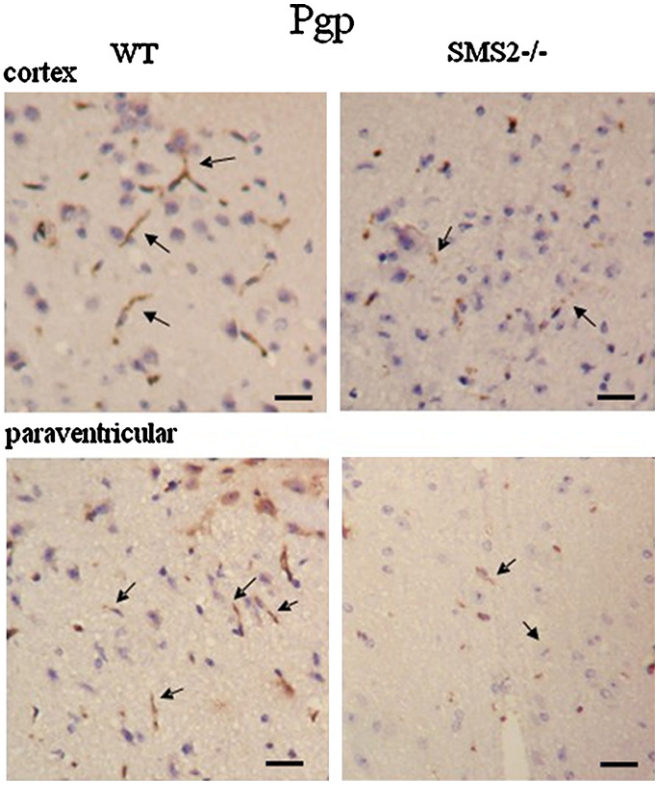

Fig. 5. Immunohistochemistry analysis of Pgp expression in WT and SMS2−/− mouse brains. The Pgp expression in both cortex and paraventricular areas of the brain tissues (250×) was revealed by 3,3′-diaminobenzidine as chromogen and the monoclonal antibody C219 for Pgp immunostaining (arrows indicate positive expression, bar = 25 μm).

4. Discussion

Primary active transporters, such as Pgp and MRP transporters, are responsible for the cellular extrusion of many kinds of drugs [25,26]. Thus, expression changes of these drug transporters either at the key barriers or within the brain are likely to have an impact on drug access and distribution to the brain. However, it is considered that the direct membrane lipid environment of the transporter is important for its expression and functionality [10,27].

In the present work, we have demonstrated for the first time that SMS2, a SMS enzyme involved in the biosynthesis of SM in mouse brain, played an important role in the regulation of Pgp expression. We found that in SMS2 deficient mouse brain, the expression of Pgp on both mRNA and protein level was significantly reduced, and the accumulation of rhodamine123 regulated by Pgp was increased accordingly. These results indicated that SMS2 deficiency efficiently downregulated Mdr1 expression and inhibited Pgp function. In addition, we demonstrated that SMS2 deficiency significantly decreased the SMS activity (around 15%) and SM levels (around 20%) in mouse brain.

Recent works have suggested the association of Pgp with cholesterol and sphingolipid-rich membrane microdomains [28,29]. However, the relationship between Pgp and SM is unknown. Our results of the 20% reduced SM levels (Fig. 1C) and more than 90% downregulated Pgp expression in SMS2

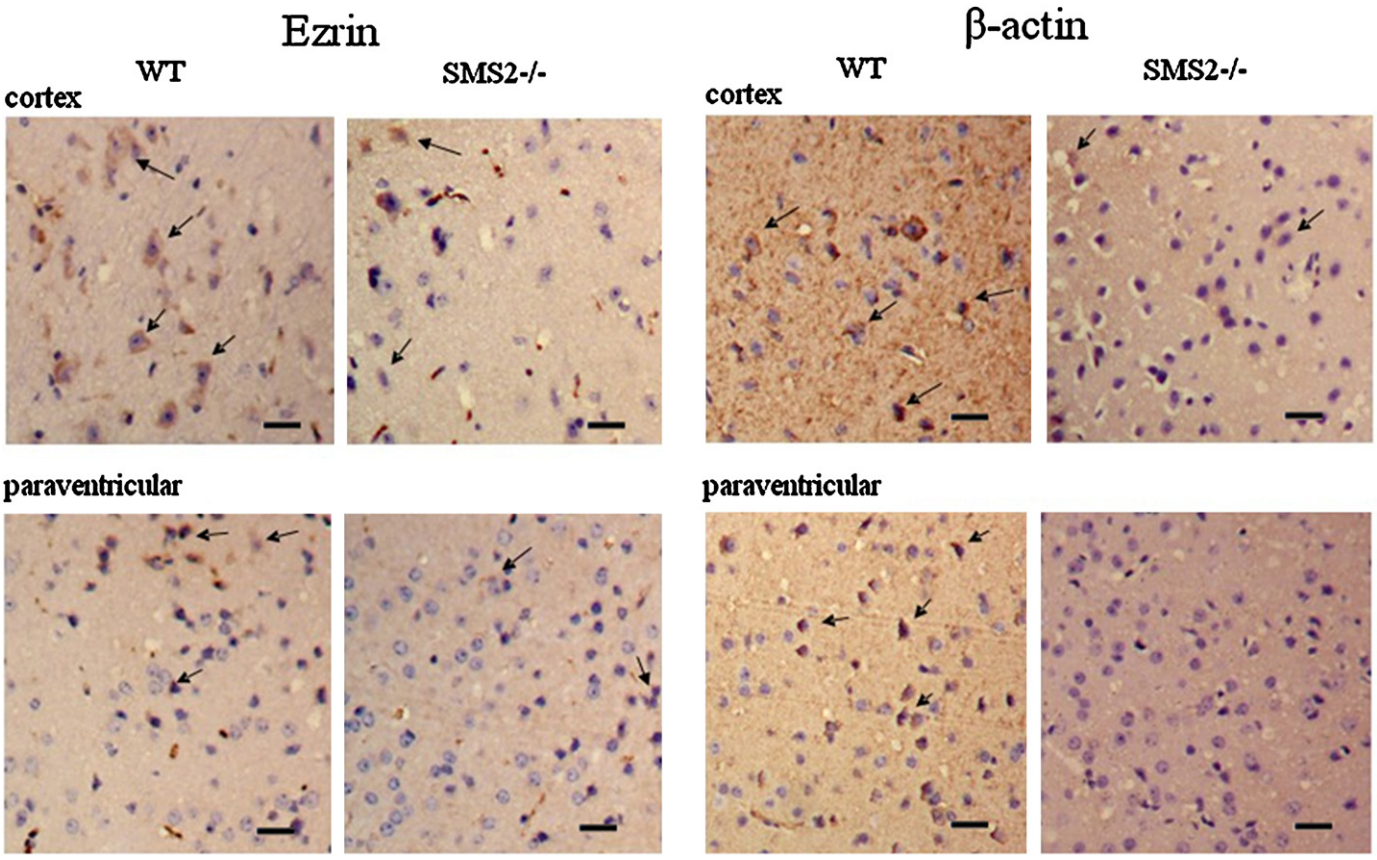

Fig. 6. Immunohistochemistry analysis of ezrin and β-actin expressionin WT and SMS2−/− mouse brains. The expression of ezrin and β-actin in both cortex and paraventricular areas of the brain tissues (250×) was revealed by 3,3′-diaminobenzidine as chromogen and anti-ezrin or anti-β-actin monoclonal antibody for the corresponding immunostaining (arrows indicate positive expression, bar = 25 μm).

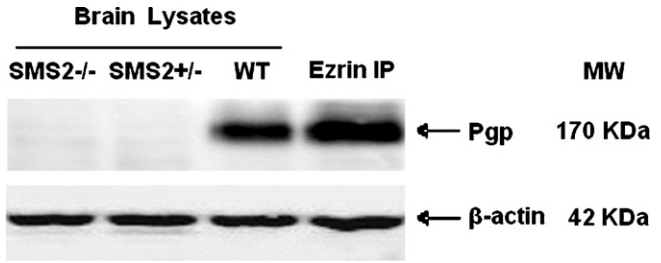

Fig. 7. Pgp–ezrin–actin association in mouse brain. Lane 1–3: brain lysates of WT, SMS2+/− and SMS2−/− mice were immunoblotted with C219 monoclonal anti-Pgp antibody using β-actin as an internal reference. Pgp was detected in WT but not SMS2 deficient mouse brain. Last lane: western blot for Pgp and β-actin in ezrin immunoprecipitates (IP) from the WT mouse brain lysates. Both Pgp and β-actin were clearly detectable in ezrin IP from WT mice brain protein.

deficient mouse brain (Fig. 3B) strongly suggested a potential functional relationship between Pgp, SM and SMS2 in the brain.

SMS2 deficiency also affected the protein expression of both ezrin and β-actin (Fig. 4C and D). Comparably, the gene expression of the other two ERM proteins of moesin and radixin was less or not affected by SMS2 deficiency in the brains (Fig. 4A). However, the protein expression of moesin was hardly detected in the mouse brain tissues, leaving questionable marks to further studies. This may also suggest that the specificity of each ERM protein; although ERM proteins were sometimes featured to be functional redundant.

Table 2
Effect of SMS2 deficiency on the brain distribution of rhodamine123.

	Rhodamine123	
	WT	SMS2−/−
Plasma level (ng/mL)	0.0146 ± 0.0004	0.0117 ± 0.0005
Brain level (ng/g brain)	0.0099 ± 0.0013	0.0693 ± 0.0016
K_p value (mL/g brain)	0.676 ± 0.088	5.905 ± 0.138

Brain-to-plasma concentration ratios (K_p) are calculated as the ratio of brain tissue concentration to plasma level. Each value is presented as mean ± SD ($n = 3$), $p < 0.05$.

Previous study by Luciani et al. had reported the interaction between Pgp, β-actin and ERM proteins in human lymphoid cell [16]. Our co-immunoprecipitation analysis results showed that both Pgp and β-actin are present in the protein sample immunoprecipitated by ezrin antibody from the total lysates of WT mouse brain (Fig. 7). Thus, this study provides an additional evidence for potential functional relationships between Pgp, β-actin and ezrin in mouse brain. It has been reported that the members of ERM proteins may associate with membrane transporters via additional coupling proteins such as PSD-95/Dlg/ZO-1 (PDZ) domain-interacting proteins [30]. It has been also proposed that the radixin, a member of ERM proteins, may bind actin filaments at its C-terminus and thus may anchor MRP2 in the membrane via a connection with actin filaments [31]. Thus, it is conceivable that in mouse brain ezrin may bind Pgp at its N-terminus not only directly, but also possibly indirectly through PDZ domain-interacting proteins, and ezrin may bind β-actin filaments at its C-terminus. Because there is the existence of such a connection between ezrin, Pgp and β-actin in mouse brain, significantly downregulated expression of Pgp results in substantial reduction of ezrin expression in SMS2 deficient mouse brain.

In conclusion, the present study suggests that SMS2 participates in regulating the expression of ABC drug transporters, and

SMS2 may be a potential target for enhancing drug access to the brain.

Conflict of interest

The authors declare no conflict of interest or financial interests.

Acknowledgments

We are grateful to Ms. Yarui Zhao and Mr. Xiaogang Wang for their assistance with breeding of the animals. We thank for Dr. Y. Hefner (1278 Avenida Miguel, Encinitas, CA 92024, USA) for helpful discussion and critical reading as well as editing this manuscript.

This work was sponsored by Shanghai Pujiang Program and National Drug Innovative Program (grant no. 2009ZX09301-011).

References

[1] Kim RB. Transporters and drug discovery: why, when, and how. Mol Pharm 2006;3:26–32.
[2] Mizuno N, Niwa T, Yotsumoto Y, Sugiyama Y. Impact of drug transporter studies on drug discovery and development. Pharmacol Rev 2003;55:425–61.
[3] Miller DS. Regulation of P-glycoprotein and other ABC drug transporters at the blood–brain barrier. Trends Pharmacol Sci 2010;31:246–54.
[4] Bauer B, Hartz AM, Miller DS. Tumor necrosis factor alpha and endothelin-1 increase P-glycoprotein expression and transport activity at the blood–brain barrier. Mol Pharmacol 2007;71:667–75.
[5] Hartz AM, Bauer B, Block ML, Hong JS, Miller DS. Diesel exhaust particles induce oxidative stress, proinflammatory signaling, and P-glycoprotein up-regulation at the blood–brain barrier. FASEB J 2008;22:2723–33.
[6] Fouassier L, Beaussier M, Schiffer E, Rey C, Barbu V, Mergey M, et al. Hypoxia-induced changes in the expression of rat hepatobiliary transporter genes. Am J Physiol Gastrointest Liver Physiol 2007;293:G25–35.
[7] McRae MP, Brouwer KLR, Kashuba ADM. Cytokine regulation of P-glycoprotein. Drug Metab Rev 2003;35:19–33.
[8] Ho EA, Piquette-Miller M. Regulation of multidrug resistance by pro-inflammatory cytokines. Curr Cancer Drug Targets 2006;6:295–311.
[9] Tchenio T, Havard M, Martinez LA, Dautry F. Heat shock-independent induction of multidrug resistance by heat shock factor 1. Mol Cell Biol 2006;26(5):80–591.
[10] Callaghan R, Berridge G, Ferry DR, Higgins CF. The functional purification of P-glycoprotein is dependent on maintenance of a lipid–protein interface. Biochim Biophys Acta 1997;1328:109–24.
[11] Kolesnick RN. Sphingomyelin and derivatives as cellular signals. Prog Lipid Res 1991;30:1–38.
[12] Huitema K, van den Dikkenberg J, Brouwers JF, Holthuis JC. Identification of a family of animal sphingomyelin synthases. EMBO J 2004;23:33–44.
[13] Li Z, Hailemariam TK, Zhou H, Li Y, Duckworth DC, Peake DA, et al. Inhibition of sphingomyelin synthase (SMS) affects intracellular sphingomyelin accumulation and plasma membrane lipid organization. Biochim Biophys Acta 2007;1771:1186–94.
[14] Liu J, Huan C, Chakraborty M, Zhang H, Lu D, Kuo MS, et al. Macrophage sphingomyelin synthase 2 deficiency decreases atherosclerosis in mice. Circ Res 2009;105:295–303.
[15] Sakai H, Tanaka Y, Tanaka M, Ban N, Yamada K, Matsumura Y, et al. ABCA2 deficiency results in abnormal sphingolipid metabolism in mouse brain. J Biol Chem 2007;282:19692–9.
[16] Luciani F, Molinari A, Lozupone F, Calcabrini A, Lugini L, Stringaro A, et al. P-glycoprotein–actin association through ERM family proteins: a role in P-glycoprotein function in human cells of lymphoid origin. Blood 2002;99:641–8.
[17] Takeshita H, Kusuzaki K, Ashihara T, Gebhardt MC, Mankin HJ, Hirasawa Y. Actin organization associated with the expression of multidrug resistant phenotype in osteosarcoma cells and the effect of actin depolymerization on drug resistance. Cancer Lett 1998;126:75–81.
[18] Kikuchi S, Hata M, Fukumoto K, Yamane Y, Matsui T, Tamura A, et al. Radixin deficiency causes conjugated hyperbilirubinemia with loss of Mrp2 from bile canalicular membranes. Nat Genet 2002;31:320–5.
[19] Yang Q, Onuki R, Nakai C, Sugiyama Y. Ezrin and radixin both regulate the apical membrane localization of ABCC2 (MRP2) in human intestinal epithelial Caco-2 cells. Exp Cell Res 2007;313:3517–25.
[20] Hailemariam TK, Huan C, Liu J, Li Z, Roman C, Kalbfeisch M, et al. Sphingomyelin synthase 2 deficiency attenuates NFkappaB activation. Arterioscler Thromb Vasc Biol 2008;28:1519–26.
[21] Meng A, Luberto C, Meier P, Bai A, Yang X, Hannun YA, et al. Sphingomyelin synthase as a potential target for D609-induced apoptosis in U937 human monocytic leukemia cells. Exp Cell Res 2004;292:385–92.
[22] Hojjati MR, Jiang XC. Rapid, specific, and sensitive measurements of plasma sphingomyelin and phosphatidylcholine. J Lipid Res 2006;47:673–6.
[23] Dong J, Liu J, Lou B, Li Z, Ye X, Wu M, et al. Adenovirus-mediated overexpression of sphingomyelin synthases 1 and 2 increases the atherogenic potential in mice. J Lipid Res 2006;47:1307–14.
[24] Patwardhan G, Gupta V, Huang J, Gu X, Liu YY. Direct assessment of P-glycoprotein efflux to determine tumor response to chemotherapy. Biochem Pharmacol 2010;80:72–9.
[25] Borst P, Evers R, Kool M, Wijnholds J, Wada M. The multidrug resistance protein family. Biochim Biophys Acta 1999;1461:347–57.
[26] Kuwano M, Toh S, Uchiumi T, Takano H, Kohno K, Wada M. Multidrug resistance-associated protein subfamily transporters and drug resistance. Anticancer Drug Res 1999;14:123–31.
[27] Klappe K, Hummel I, Hoekstra D, Kok JW. Lipid dependence of ABC transporter localization and function. Chem Phys Lipids 2009;161:57–64.
[28] Lavie Y, Fiucci G, Liscovitch M. Up-regulation of caveolae and caveolar constituents in multidrug-resistant cancer cells. J Biol Chem 1998;273:32380–3.
[29] Barakat S, Gayet L, Dayan G, Labialle S, Lazar A, Oleinikov V, et al. Multidrug-resistant cancer cells contain two populations of P-glycoprotein with differently stimulated Pgp ATPase activities: evidence from atomic force microscopy and biochemical analysis. Biochem J 2005;388:563–71.
[30] Short DB, Trotter KW, Reczek D, Kreda SM, Bretscher A, Boucher RC, et al. An apical PDZ protein anchors the cystic fibrosis transmembrane conductance regulator to the cytoskeleton. J Biol Chem 1998;273:19797–801.
[31] Kojima H, Nies1 AT, König J, Hagmann W, Spring H, Uemura M, et al. Changes in the expression and localization of hepatocellular transporters and radixin in primary biliary cirrhosis. J Hepatol 2003;39:693–702.